Chapter 2

Synthesis and Characterization Techniques

2.1 Overview

This chapter deals with the description of the research techniques used for the synthesis and characterization and electrode preparation techniques and electrochemical measurements of different types of materials developed by tuning of Redox energies of transition metal- ion in different lattices for energy storage applications.

Different types of morphologies have been discussed in this chapter. Fundamentals related to different characterization techniques like XRD, SEM, TEM, TGA FTIR, Raman, and UV-visible absorption spectroscopy and Electrochemical characterization(cyclic voltammetry (CV), LSV(Linear swept voltammetry), Electrochemical Impedance Spectroscopy(EIS), Chronoamperometry charge-discharge) have been discussed in details in this chapter.

2.2 Materials Synthesis techniques

Different types of synthesis techniques have been presented in detail in this section. Mainly three different synthesis routes were followed in this thesis. The schematic representation of the three routes is explained in **Figure 2.1**.
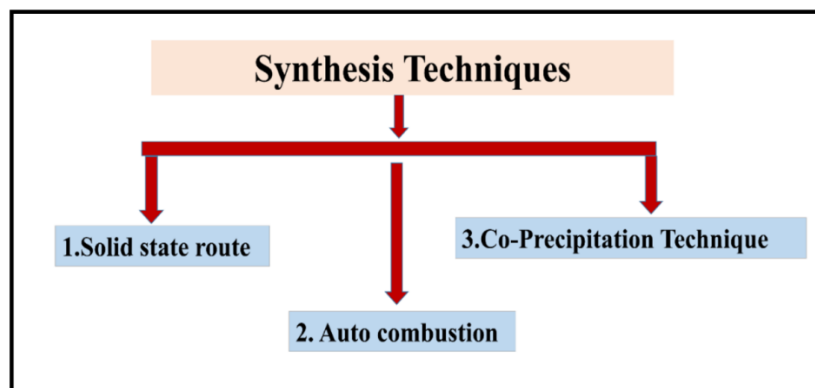

Figure 2.1 Schematic representation of the three types of synthesis routes

2.2.1 Solid-state or Ceramic method

The solid-state reaction is the route of the synthesis process for synthesizing polycrystalline material from solid reagents. The reaction occurs at a very high temperature. Factors that affect solid-state reaction are chemical and morphological properties of the reagents including the reactivity, surface area, and free energy change with the solid-state reaction, and other reaction conditions, such as the temperature, pressure, and the environment of the reaction. The advantage of the method is large-scale production.[1] A detailed block diagram in **Figure 2.2** shows the steps involved in the synthesis.
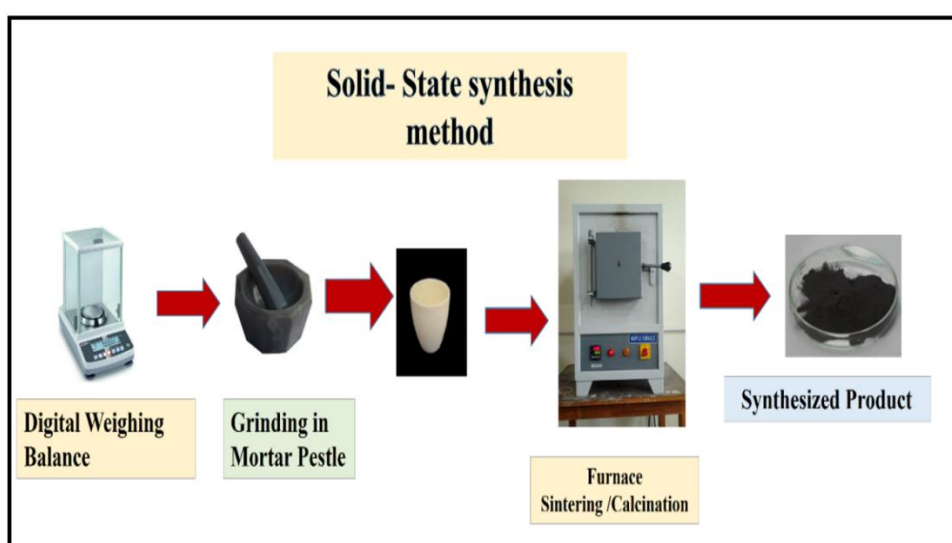

Figure 2.2 block diagram of solid-state synthesis process or Ceramic method

2.2.2 sol-gel auto combustion method

Sol-gel auto combustion is a fast and cost-effective synthesis technique, a variety of metal oxide and nanoparticles are synthesized in this process. advantage of this process is synthesized nano-sized, homogeneous, and highly mixed different elements at the atomic level. Here different types of fuel are used for the auto-combustions process and comparative low-temperature desired products can be synthesized.[2] citric acid ($C_6H_8O_7$), dextrose ($C_6H_{12}O_6$), sucrose ($C_{12}H_{22}O_{11}$), urea (CH_4N_2O), glycine ($C_2H_5NO_2$), etc are commonly used as fuels in the sol-gel auto combustion process. Urea, glycine, and citric acid make strong complexes with metal cations in the solution. These fuels take part in two purposes; (1) during combustion form CO_2, and H_2O, which liberate heat in the exothermic process, and (2) the form complexes with

metal ions simplifying the homogeneous mixing of the cations in solution. Since nitrogen itself does not participate in the redox reaction it is thought that it is released as a gaseous substance increasing the porosity of the obtained materials. The intensity of the combustion reaction is also dependent on the type of fuel [3] A detailed block diagram in **Figure 2.3** shows the steps involved in the synthesis process.
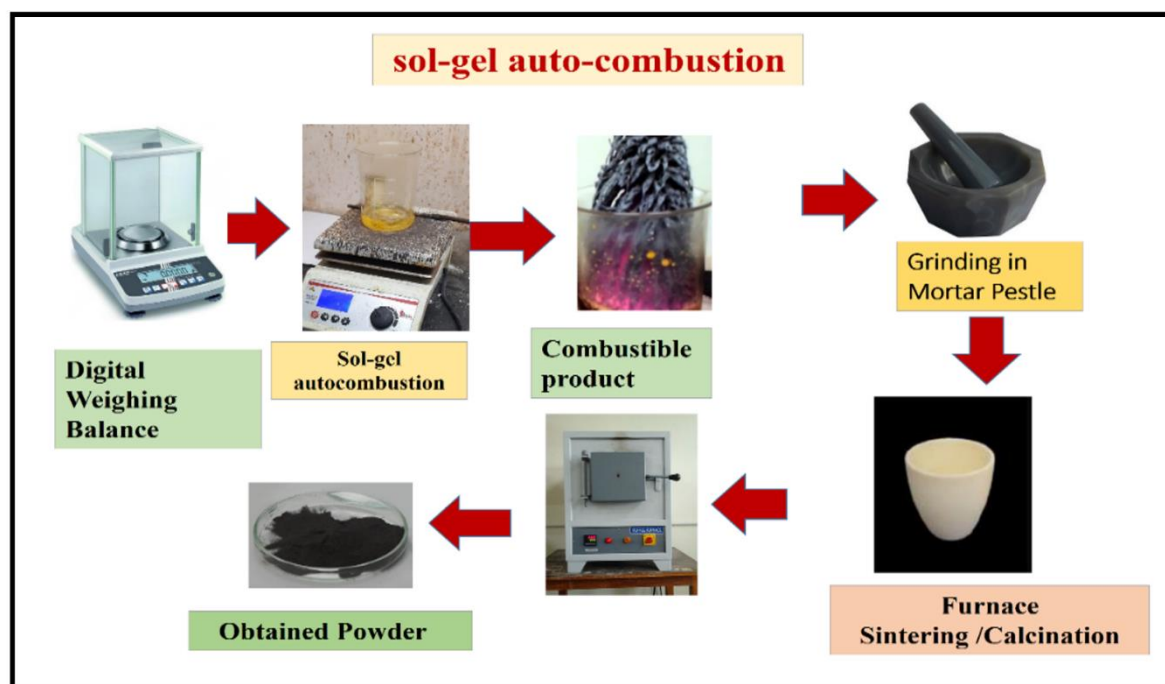

Figure 2.3 block diagram sol-gel auto combustion synthesis process

2.2.3 Co-precipitation method

The coprecipitation technique involves the precipitation of metal in the form of hydroxide or oxalate from a salt precursor with the help of a base in a solvent. monodispersed nanoparticles synthesized by controlled release of anions and cations assist the nucleation and particle growth kinetics[4]. The control of chemical homogeneity and particle size is difficult in mixed oxide precipitation for this reason some modifications are taken, such as the application of surfactants, sonochemical methods, and high-gravity reactive precipitation that helps to regulate the morphological characteristics properly. The appropriate control of experimental parameters, such as pH, the concentration of the reactants and ions, and temperature

are important parameters of the precipitation process [5] A detailed block diagram in **Figure 2.4** shows the steps involved in the synthesis.
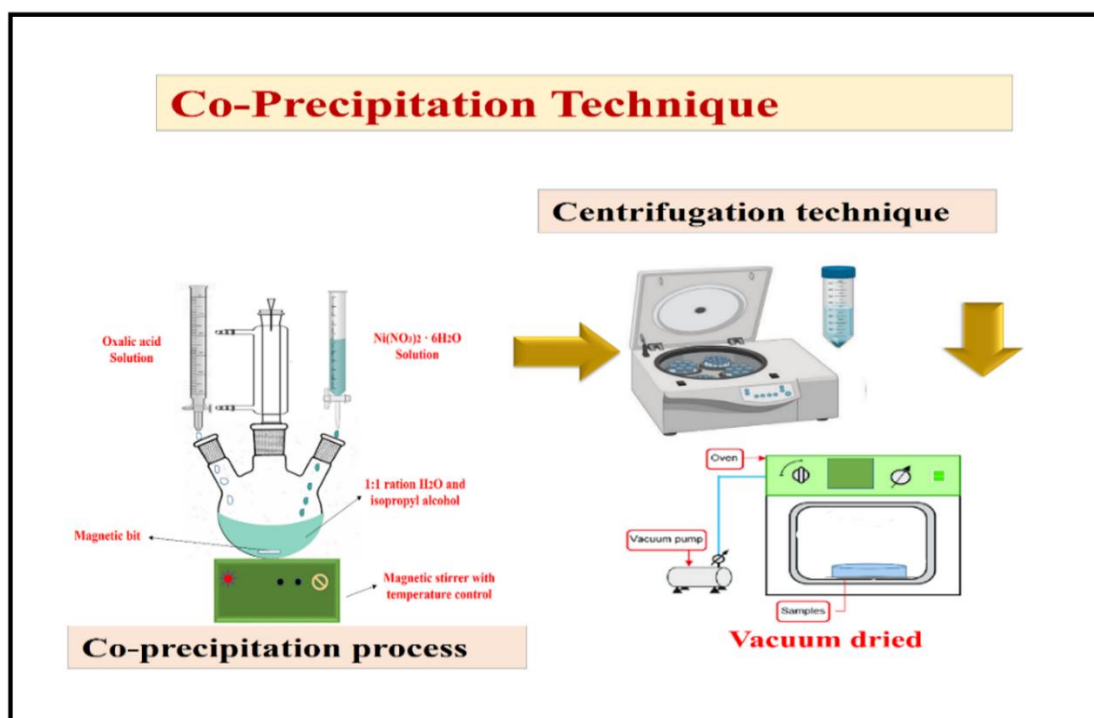

Figure 2.4 block diagram Co-precipitation synthesis process

2.3 Characterization Techniques

2.3.1 X-ray Diffraction (XRD)

X-ray diffraction (XRD) is a non-destructive technique used to identify the structural properties of materials. In this characterization technique, an electromagnetic wave of the wavelength of ~1 Å is diffracted from the crystal lattice planes oriented in distinct directions in the crystal due to comparable order of magnitude of the X-rays wavelength and crystal lattice.

The X-ray diffractometer consists of three basic components-

a) X-ray tube

b) A sample holder

c) X-ray detector

X-rays are generated in a cathode ray tube (CRT) by heating a filament to generate electrons. These electrons are accelerated by applying voltage and having certain

energy to eject out the inner shell electrons of the target. During that time the characteristic X-rays are generated from the target having different components K_α and K_β. The K_α consists of two wavelengths, $K_{\alpha 1}$ and $K_{\alpha 2}$. $K_{\alpha 1}$ has a slightly shorter wavelength and double the intensity of $K_{\alpha 2}$. The filter is used to produce the monochromatic X-ray. The XRD works on the principle of Bragg's law, which suggests that constructive interference will be resulting in an intense peak when the path difference between the waves is an integral multiple of the X-ray wavelength. Bragg's law can be expressed as follows-

$$2d_{hkl}Sin\theta = n\,\lambda \qquad\qquad (2.1)$$

Where the interplanar distance is d_{hkl} (h, k, l are Miller indices) and θ represents Bragg's angle[6,7]. The order of diffraction is n ($n = 1$ for XRD) and λ is the wavelength of the X-Ray. **Figure 2.6** is the illustration of Bragg's law. The diffraction peaks depend upon the symmetry of the structure of the materials.
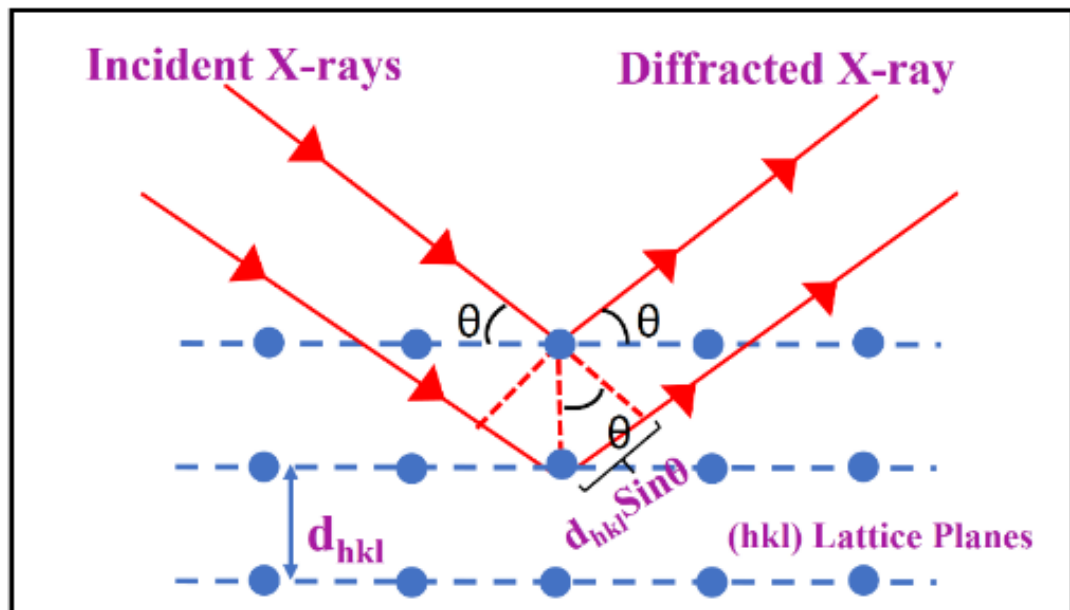

Figure 2.5 Schematic diagram of the incident and diffracted X-rays from the crystal.[6]

Figure 2. 6 Rigaku, Miniflex II, Japan, IIT (BHU) Varanasi

2.3.2 High-Resolution Scanning Electron Microscopy (HR-SEM)

Electron microscopy has been a revolutionary imaging technology widely used by the scientific and engineering community to observe the morphology and structure of nanomaterials. The Nova NanoSEM 450 scanning electron microscope (SEM) was employed to understand the morphology of the prepared sample. In the SEM technique, an electron beam is focused with the help of different magnetic lenses and apertures on the sample to create an image. In this measurement technique, the specimen needs to be electronically conducting to avoid the charging effects, which produce blur image quality at high resolutions. **Figure 2.7** shows the typical layout of HR-SEM, which consists of an electron gun from where the electrons are generated and accelerated via an accelerating anode, electromagnetic lenses for focussing the electrons, a vacuum chamber, and a detector to collect the signals emitted from materials [8]. The scattering occurs due to interaction between the high-energy electrons and the specimen, which results in the generation of different signals such as secondary electrons, backscattered electrons, characteristic X-rays, and auger electrons. The Auger electrons are generated from the surface of the sample in a low atomic number molecule.
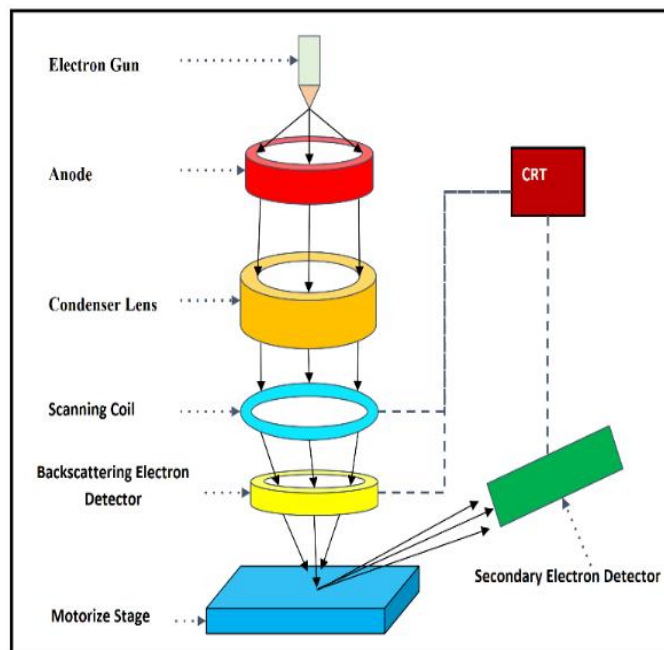
Figure 2.7 Schematic diagram of the core component of SEM microscopy [9].

The secondary electrons are generated by the inelastic scattering and they have energy around a few keV and backscattered electrons are generated by elastic scattering and have high energy. The imaging is done with the improved spatial resolution by the secondary electron [8-9]. The image quality in SEM depends on the depth of field and the resolution, which can be affected by working distance, probe current, accelerating voltage, and astigmatism. The resolution in SEM is in the nanometer range. **Figure 2.8** shows a picture the of HR-SEM

Figure .2.8 HR-SEM Instrument facility, ZEISS EVO 18 in CIFC IIT (BHU) Varanasi

2.3.3 High-Resolution Transmission Electron Microscopy (HR-TEM)

High-Resolution Transmission electron microscopy (HR-TEM) has been widely used to characterize nano and bulk materials. It is an electron microscopy technique, where the incident electron beam is transmitted through the material to generate a two-dimensional (2D) image. The FEI Tecnai G2 20 TWIN TEM was employed to observe the thickness and the selective area electron diffraction (SAED) pattern of the prepared sample. In TEM, like SEM, an electron beam is focused with the help of different magnetic lenses and apertures on the sample. However, in HR-TEM, electrons are transmitted through the specimen and they arrive at a detector below the sample to produce a 2D image of the specimen. This image gives detailed information about the sample's morphology, composition, and crystal structure[9-10].

The typical layout of HR-TEM is shown in **Figure 2.9 (a)**, where the objective aperture is placed in the back focal plane of the objective lens. Transmitted and diffracted electrons are used by changing the aperture position for the bright-field and dark-field imaging modes in TEM as shown in **Figure 2.9 (b)** and **Figure 2.9 (c),** respectively

The transmitted electrons can pass through the aperture in bright-field mode and the obtained images depict mass-thickness contrast. However, in the dark-field mode, the transmitted electrons are fully blocked by the aperture and diffracted electron beam is allowed to pass through the aperture, which provides information about the crystal structure. [9,11] In TEM, the specimen needs to be ultrathin (less than 100 nm) or a suspension of the material on a grid. The TEM has the highest resolution (atomic level) of any electron microscope and it has a magnification of 10 to 50 million times. **Figure 2.10** shows the HRTEM instrument installed in CIFC, IIT(BHU) Varanasi
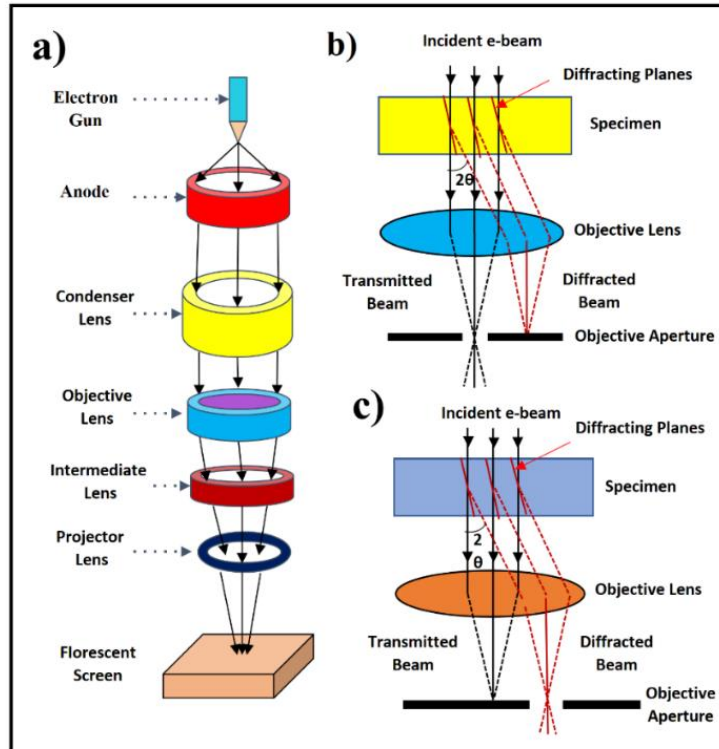
Figure 2.9 (a) Schematic diagram of core component of TEM microscopy. Transmitted and diffracted electrons for (b) Bright field and (c) Dark field imaging in TEM [9] (Figure is taken from open access internet source)

..

Figure 2.10 HRTEM Facilities with EDAX spectrometer, IIT (BHU) Varanasi

2.3.4 Thermogravimetric analysis (TGA)

The TGA analysis technique, in general, is used to determine the thermal stability of the different types of oxide nitride and sulfide materials. In this method, the mass of the sample is recorded as a function of temperature, which is used to take information about the change in mass (absorption or desorption), phase transition, and thermal decomposition. If the mass of the sample remains constant in a given temperature range, then the sample is said to be thermally stable in that range. TGA also helps to determine the calcination temperature of the sample as it provides the upper limit of temperature beyond which degradation of the sample starts. [12] **Figure 2.11** shows a picture of the TGA measurement system installed at IIT(BHU) Varanasi.

Figure 2.11: TGA measurement system CIFC, IIT (BHU) Varanasi

2.3.5 Fourier transform infrared (FTIR) spectroscopy

FTIR produces an infrared absorption spectrum to help of spectrum identify the presence of certain functional groups in a molecule. The spectrum of distinct molecular fingerprints can be used to screen and scan samples for many different components. FTIR detects functional groups and characterizes covalent bonding

information. An FTIR spectrometer consists of a light source, monochromatic, slit, beam splitter, detector, and an analog recorder. The monochromator (e.g., a salt prism or grating with finely spaced lines) differentiates the source radiation into its different wavelengths. The slit selects the collection of wavelengths that pass through the sample at any given time. In a double-beam operation, a beam splitter separates the incident beam in two; half goes to the sample and half to the reference. The sample absorbs light according to its chemical properties. The detector collects the radiation that passes through the sample and compares its energy to that going through the reference. The detector produces an electrical signal. A link between the monochromator and the detector allows the user to record energy as a function of frequency or wavelength. To improve the resolution, it is necessary to narrow the slit and decrease the sensitivity. Secondly, it is possible to run multiple scans to build up a signal-to-noise ratio. Finally, the instrument needs to be calibrated repetitively due to misalignment between the analog connection and the monochromator.[13-14] **Figure 2.12** shows the mechanism of FTIR and **Figure 2.13** shows the FTIR spectrometer installed at CIFC, IIT(BHU) Varanasi.
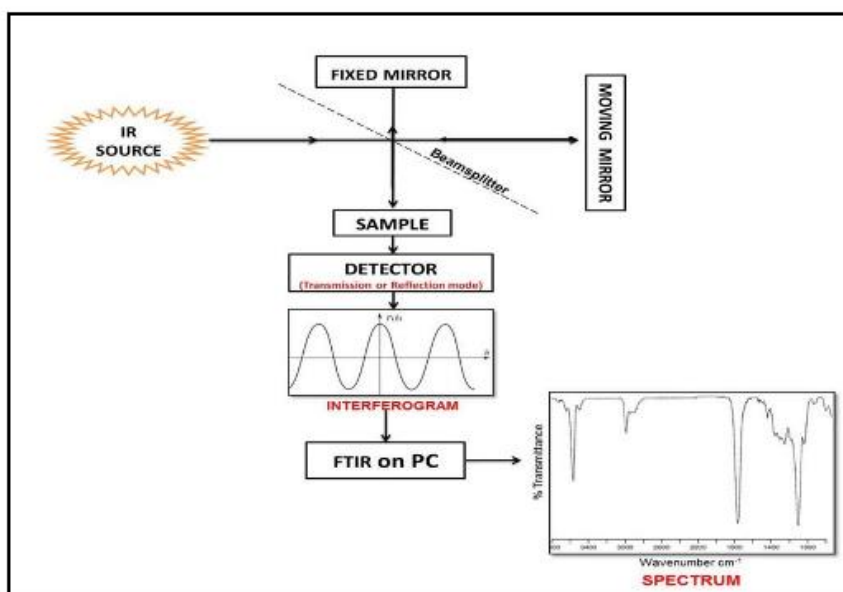

Figure2.12: Brief mechanism of FTIR for detection [14] (Figure is taken from open access internet source)
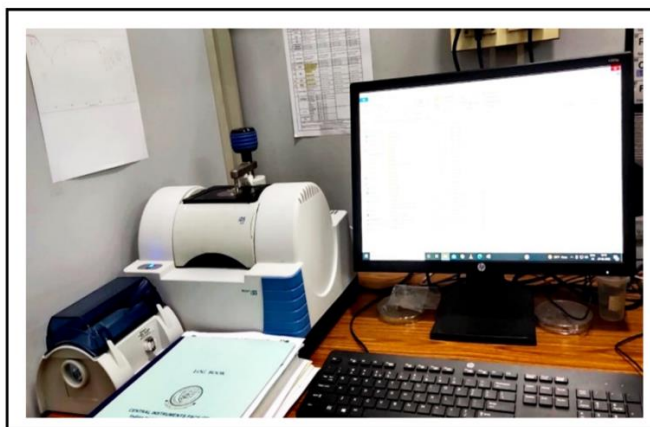
Figure 2.13 FTIR spectrometer CIFC, IIT (BHU) Varanasi

2.3.6 UV-Visible Spectroscopy

This is a useful technique to determine the band gap and the absorption properties of materials within the visible and adjacent (near-ultraviolet and near-infrared) range. A compound absorbs light in the UV-visible region and gets excited and the absorption spectra are used to determine the bandgap of the semiconductors. The absorbance is measured with respect to a reference and a graph of absorbance vs wavelength is plotted [15]. The schematic diagram of the UV-visible spectrophotometer is shown in **Figure 2.13**. In this study difference between absorbed light intensities of sample and reference cell is measured to identify the absorption characteristic of the sample
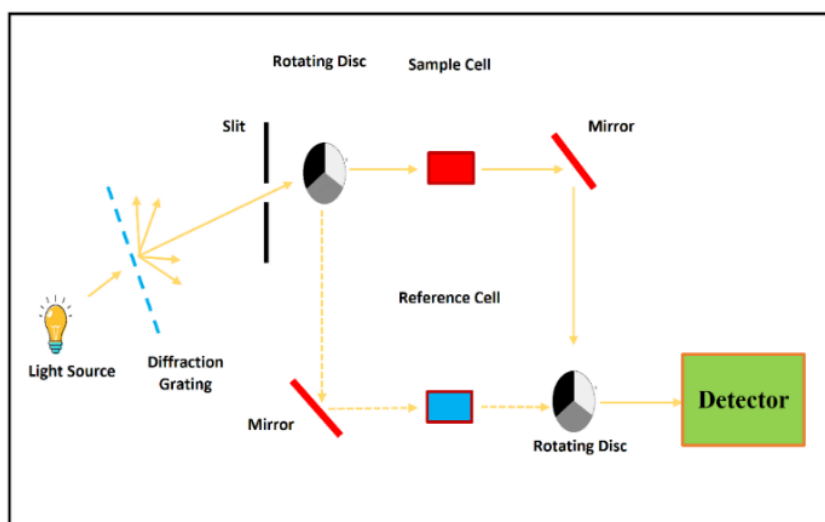

Figure 2.14 Schematic diagram of UV-Visible spectrometer [15].

2.3.7 Raman Spectroscopy

Raman spectroscopy is a non-destructive powerful tool to characterize materials. Raman spectroscopy has been widely used to figure out the layer number and the defect in 2D materials. The basic principle of Raman spectroscopy is based on the interaction between electromagnetic field (EMF) and materials/molecules, which results in inelastic scattering. The incident EMF i.e. photons interact with the analytic molecule, and a dipole moment is induced which is directly proportional to the polarizability of the molecule. The magnitude of induced dipole moment (μ_{ind}) depends on the strength of the incident electric field (E_{in}) and the polarizability of the molecule (α_m) and it can be expressed as follows [16]

$$\mu_{ind} = E_{in}(\omega_{inc}).\alpha_m \tag{2.2}$$

In the Raman scattering process, the incoming photons are not absorbed by the molecule rather they are scattered. The scattered photon frequency is proportional to the difference in energy of the molecular vibrational levels. The classical theory explained the inelastic scattering of incident electric field E_{in} and the angular Eigen frequency (ω_{vib}) of the vibrating molecule. This interaction results in three dipole components $\mu_{ind}(\omega_{inc})$, $\mu_{ind}(\omega_{inc} - \omega_{vib})$ and $\mu_{ind}(\omega_{inc} + \omega_{vib})$ corresponding to Rayleigh, Stokes, and Anti-Stokes, respectively, as shown in **Figure 2.15**.
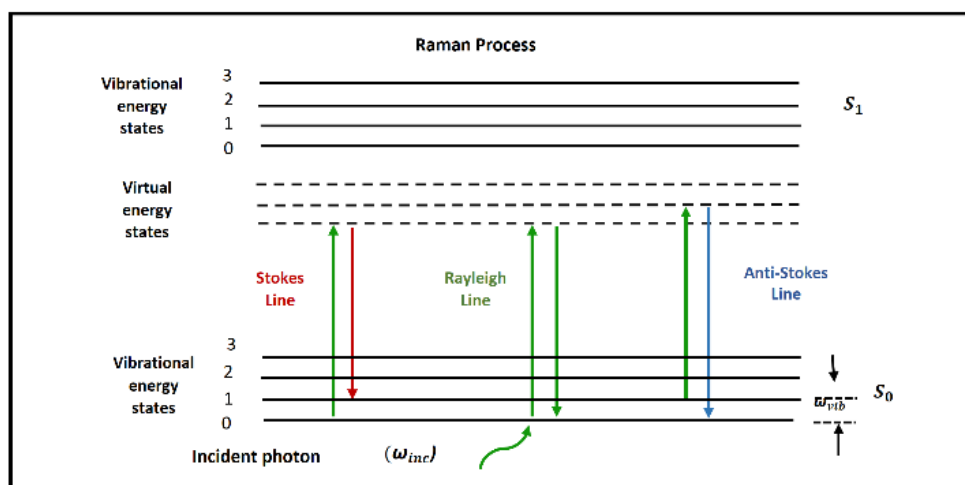

Figure 2.15 Schematic representation of the scattering process in Raman scattering (Rayleigh, stokes, and anti-stokes line) [17]. (Figure is taken from open access internet source)

61

The shorter wavelength laser possesses higher Raman scattering (inelastic scattering) cross-sections; hence it provides a greater signal. In Raman's study, inelastic scattering occurs when the incident photon wavelength is different from the scattered photon wavelength, the higher wavelength is stoked and the lower wavelength is the anti-stokes lines. The intensity of the Raman signal is very weak as compared to the incident laser, i.e., single inelastic scattering out of one million scatterings. A Raman spectrometer has mainly three components such as laser, the sampling interface, and the spectrometer as shown schematically in **Figure 2.16** In the Raman system, fiber optics cables have been used to transmit and collect the signal from the specimen. To remove the Rayleigh signals, a notch filter is used and the remaining signals are passed through a dispersive holographic grating. To reduce the intensity of the incident monochromatic laser source, we have used a different neutral density filter. To detect the Raman signal, a high-quality CCD detector is used. [16-18]
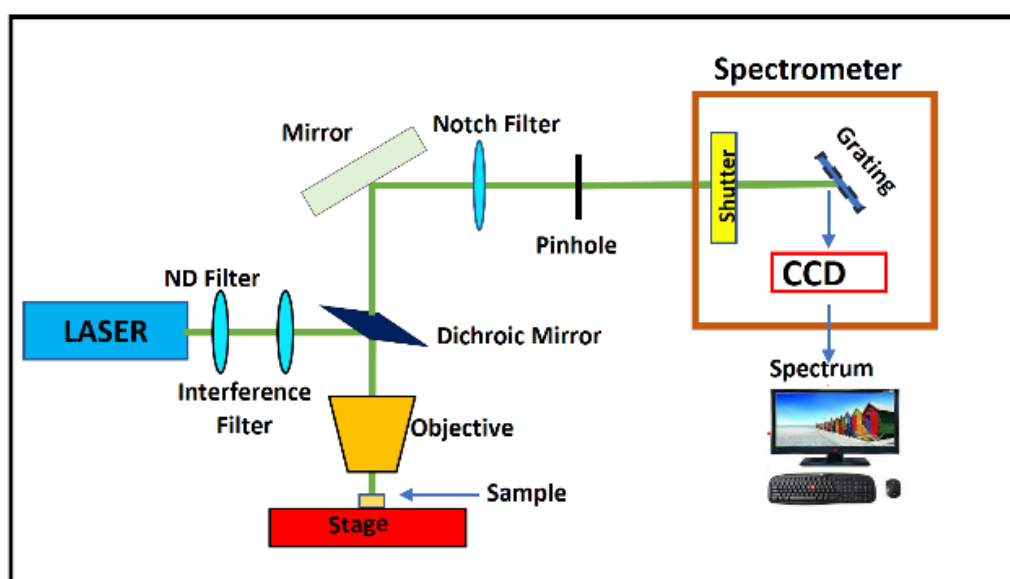

Figure 2.16 Schematic diagram of Raman spectrometer.

2. 3.8 X-ray Photoelectron Spectroscopy (XPS)

X-ray photoelectron spectroscopy (or XPS) is widely used to investigate the chemical composition of surfaces. X-ray Photoelectron Spectroscopy (XPS) is based on the photoelectric effect. The surface of a solid has a different chemical composition and physical properties from the interior of the solid. An intense beam of ultraviolet or X-ray light ionizes the molecules or atoms. The light used must have an energy

sufficient to ionize electrons at least from the highest valence shell of atoms. XPS technique involves hitting the sample with low energy ((~1.5 Kev) X-rays such that a photoelectric effect is induced. An electron spectrometer with high resolution records the energy spectrum of emitted photoelectron. When photons of known energy (usually X-rays) hits the surface, an electron from K-shell is knocked out; the kinetic energy (K.E.) of this electron is studied in spectroscopy. The spectrum is displayed as a plot of the binding energy as a function of the electron counting rate. Binding energy is one unique characteristic of each element. While striking with x-ray we keep the depth of penetration in solids limited to a few microns Thus, interactions take place between the incident photons and the surface atoms leading to the photoelectric emission of electrons. **Figure 2.17** represent the mechanism of XPS.
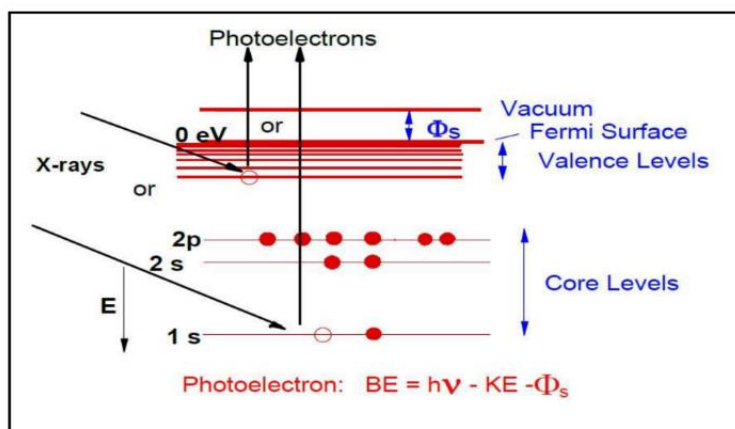

Figure 2.17 : Schematic diagram XPS Basic Principle[19] (Figure is taken from open access internet source)

Figure 2.18 XPS Spectrometer, CIFC. IIT (BHU) Varanasi

The kinetic energy of the electrons ejected can be expressed as:

$$\text{Kinetic Energy (K.E.)} = h\nu - \text{B.E.} - \phi S \qquad (2.3)$$

Where $h\nu$ = energy of the photon, B.E. = binding energy of the atomic orbital from which the electron is ejected, and ϕS = work function of spectrometer. In the XPS spectrum, the innermost orbital appears at higher binding energy than the outer orbital. Binding energies of 1s orbitals are proportional to atomic number and increase with it with some empirical formula. [19] **Figure 2.18** shows the XPS Spectroscopy instrument.

2.3.9 BET (Brunauer, Emmett, and Teller) specific surface area analysis

Brunauer-Emmett-Teller (BET) analysis, which is based on the Langmuir isotherm theory for monolayer adsorption, was developed in 1938 by Stephen Brunauer, Paul Hugh Emmett and Edward Teller.[20] BET analysis is useful for obtaining structural information of the catalyst and its support, especially when the material is porous. Typically, the physical adsorption of noncorrosive gas molecules (N_2, Ar, CO_2, etc.) onto the surface of solid material is utilized to measure the specific surface area, average pore volume, and pore size distribution of the sample. The theory works based on several assumptions, which are from Langmuir isotherm theory: 1) Adsorption occurs only on well-defined sites of the sample. 2) There is no interaction between each adsorption layer. 3) Adsorption occurs as a monolayer and each layer is treated as a Langmuir monolayer. Based on the above assumptions, the following BET equation has been used:

$$\frac{1}{v\left[\frac{p_0}{p}-1\right]} = \frac{c-1}{v_m c}\left(\frac{p_0}{p}\right) + \frac{1}{v_m c} \qquad (2.4)$$

Where p and p_0 are the equilibrium and saturation pressure of the adsorbents at the temperature of adsorption, v is the adsorbed gas quantity, and v_m is the monolayer adsorbed gas quantity. c is the BET constant, which is defined as:

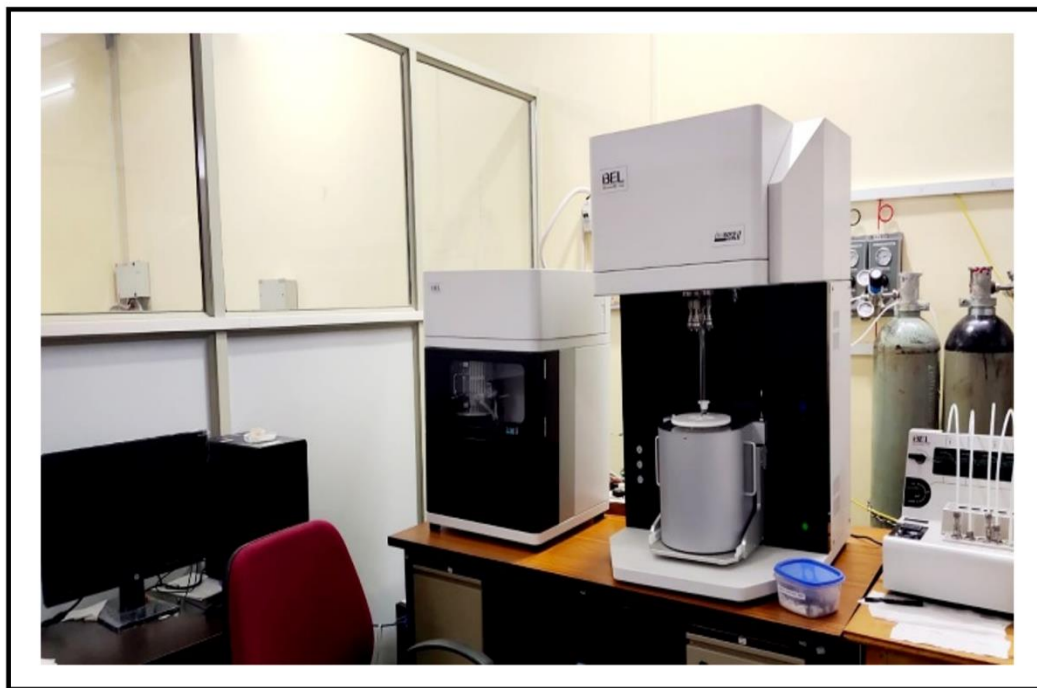$$c = \exp(\frac{E_1 - E_L}{RT}) \qquad (2.5)$$

Figure 2.19: BET surface area measurement system, CIFC, IIT (BHU) Varanasi

Where E_I is the heat of adsorption for the first layer and E_L is the heat of adsorption for the next layers. By adjusting the pressure, the equation can be modified and plotted as a linear relationship. An intercept and a slope from the plot provide the volume of adsorbed gas in the monolayer (νm). Then νm is utilized to calculate the specific surface area according to the following equations

$$S_{Total} = \frac{(v_m N_s)}{V} S_{BET} = \frac{S_{Total}}{a} \qquad (2.6)$$

Where N is the Avogadro's number, s is the adsorption cross-sections of the adsorbing species and α is the mass of the solid sample or adsorbent. [21] **Figure 2.19** shows XPS Spectroscopy

2.4 Electrode Fabrication and Cell Assembly

2.4.1 Electrode fabrication

The active materials (different types of oxide materials utilized in the study), carbon black and polyvinylidene fluoride (PVDF) powders are pre-weighed before mixing them. The three ingredients are ground thoroughly in a mortar followed by the

addition of a small amount of N-methyl pyrrolidinone (NMP) solution to form a slurry. For supercapacitor application, the slurry is then applied (area of coating: 1 cm^2, and a total mass of around 1 mg) uniformly onto carbon Torry paper with help of a micropipette. The fabricated electrodes are immediately transferred to an electric oven and dried at 90° C under vacuum overnight. **Figure 2.20** shows the prepared electrode for the study.

Figure 2.20: electrode picture for supercapacitor application

2.4.2 Cell Assembly

For the electrocatalyst (OER and ORR) test beaker-type three-electrode cell was assembled with a working electrode facing a counter electrode (platinum wire) and reference electrode (saturated calomel electrode, SCE or Hg/HgO, Ag/Ag$_2$Cl$_2$) in his study 1-6 M KOH were used as an electrolyte.

For the supercapacitor performance test, the beaker-type three-electrode cell was assembled with a working electrode facing a counter electrode (platinum wire) and reference electrode (saturated calomel electrode, SCE or Hg/HgO, Ag/Ag$_2$Cl$_2$), which was placed close to the working electrode. In this study, 2 M KOH and 0.5 to 1 M Na$_2$SO$_4$ were used as an electrolyte. Before electrochemical testing, the three-electrode cell was left for one or two hours so that the electrolyte solution can penetrate the working electrode. **Figure 2.21** shows three-electrode cells utilized in the study.
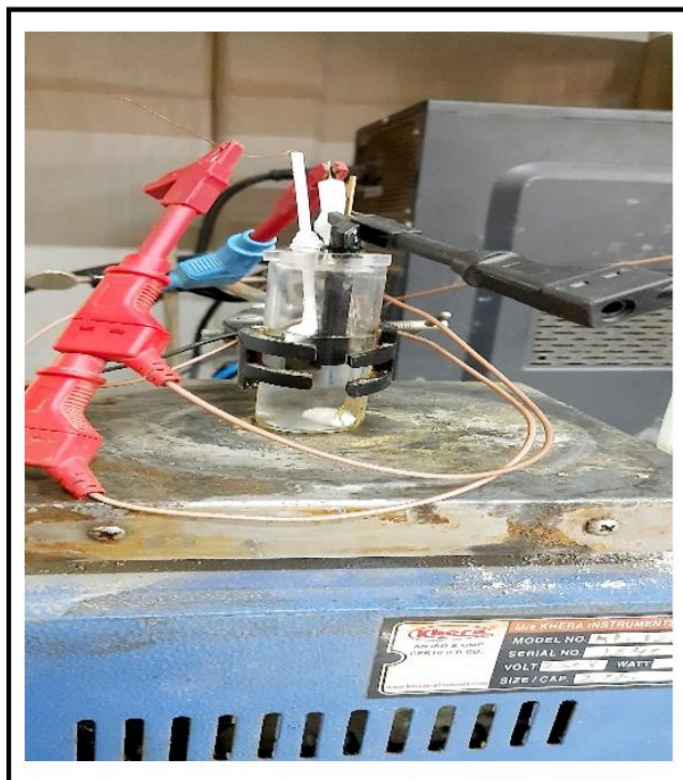
Figure 2.21 electrochemical cell in a three-electrode system

2.4.3 Electrochemical characterization techniques

Electrochemistry is a branch of chemistry that studies chemical reactions that take place in a solution at the interface of an electron conductor and an ionic conductor, and which involve electron transfer between the electrode and the electrolyte or species in solution. In this study, the electrochemical properties were evaluated by linear sweep voltammetry (LSV), cyclic voltammetry, galvanostatic charge-discharge, and electrochemical impedance spectroscopy, which are discussed below.

2.4.3.1 Linear sweep voltammetry (LSV)

For OER and ORR applications LSV measurement was used, Linear sweep voltammetry (LSV) can identify unknown species and determine the concentration of solutions. , LSV was conducted on an Autolab instrument (model no. PGSTAT204), A fixed potential range is employed and the voltage is scanned from a lower limit to an upper limit, as shown in **Figure 2.22.** The slope of the potential vs time graph is called the scan rate and can range from 1 mV/s to 10^3 V/s. The characteristics of LSV depend on several factors, including the rate of the electron transfer reactions, the chemical reactivity of the electroactive species, and the scan rate. LSV measurement, the current response is plotted as a function of the voltage.

The equation below gives an example of a reduction occurring at the surface of the working electrode.

$$O + e^- \leftrightarrow R \qquad (2.7)$$

Assuming E_i is the reduction potential of O in a standard condition, as the voltage is swept from E_i to E, a current begins to flow, and [O]=[R] (concentration of the redox species) at the surface when $E = E_i$. As the molecules on the surface of the working electrode are reduced, they move away from the surface and new molecules come into contact with the surface of the working electrode. The flow of electrons into or out of the electrode causes the current. The current is a direct measure of the rate at which electrons are being exchanged through the electrode-electrolyte interface. When this rate becomes higher than the rate at which the oxidizing or reducing species can diffuse from the bulk of the electrolyte to the surface of the electrode. [20]
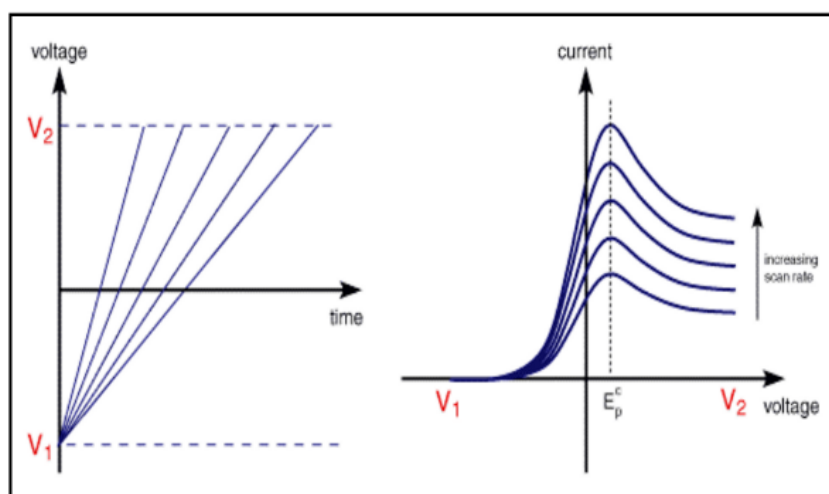

Figure 2.22 : Linear sweep voltammetry (LSV) polarization curve , voltage(V) vs. current [20] (Figure is taken from open access internet source)

2.4.3.2 Cyclic voltammetry (CV)

Cyclic voltammetry (CV) is a powerful and popular electrochemical technique commonly employed to investigate the reduction and oxidation processes of molecular species. CV is also invaluable to study electron transfer-initiated chemical reactions, which include catalysis. Electrochemical redox of electrode surface study was done by Cyclic voltammetry (CV) Pseudocapacitor behavior and ORR/OER catalytic activity both were studied by CV. In this whole research dissertation, CV was conducted on an Autolab instrument (model no. PGSTAT204) at different scan rates and voltage ranges at room temperature. CV is the most widely used technique for acquiring qualitative information about the electrochemical

reactions in **figure 2.23.** It offers rapid identification of redox potentials of the electroactive species. A typical electrode reaction involves the transfer of charge between an electrode and a species in the solution. The electrode reaction is usually referred to as electrolysis, which typically involves a series of steps. CV is very similar to LSV. In this case, the voltage is swept between two values at a fixed rate; however. The forward sweep produces an identical response to that seen for the LSV experiment. The current flow in reverse is from the solution species back to the electrode and, therefore, occurs in an opposite sense to the forward step, but otherwise, the behavior can be explained identically.[20-22]
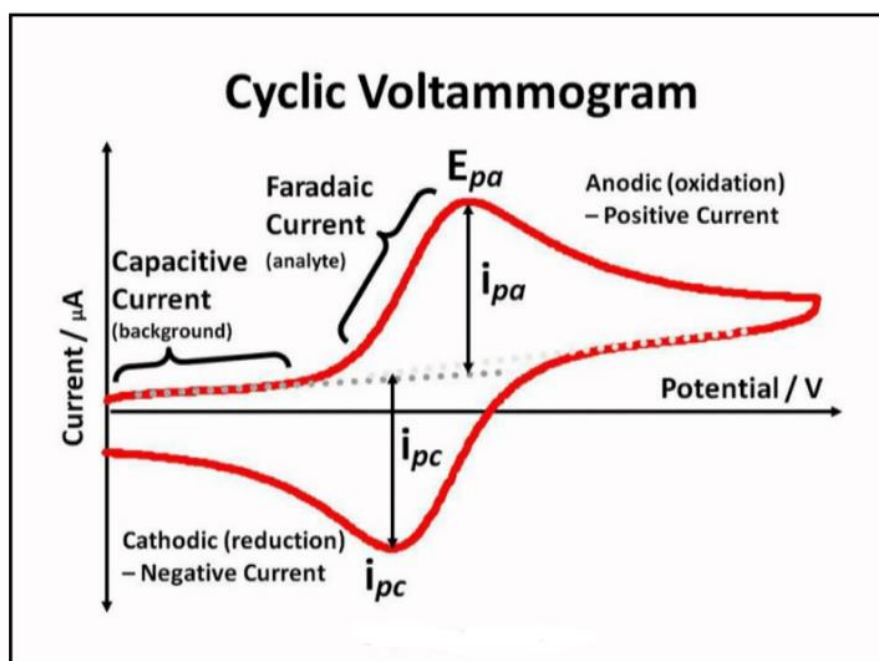

Figure 2.23 : Cyclic voltammetry (CV) polarization curve , voltage(V) vs. current [22] (Figure is taken from open access internet source)

2.4.3.3 chemical Kinetic for pseudocapacitors from Cyclic voltammetry (CV) curve

The type of supercapacitor can be distinguished by Current-Voltage response, This section discusses the kinetics of pseudocapacitance from cyclic voltammetry polarization curve,

1. Linear or pseudo linear relationship between the applied potential and state of charge (capacitance, dQ/dV)

2. Nearly ideal electrochemical reversibility

3. Surface-controlled kinetics

Lindström et al. Studied kinetics of Li^+ insertion into nano, porous anatase TiO_2 films and they found a relationship between the applied sweep rate and observed electrochemical current, they introduced b-value analysis. b value determine the presence of surface controlled/ capacitive (vs. semi-infinite diffusion-controlled) kinetics:[23]

$$i(V) = av^b \tag{2.8}$$

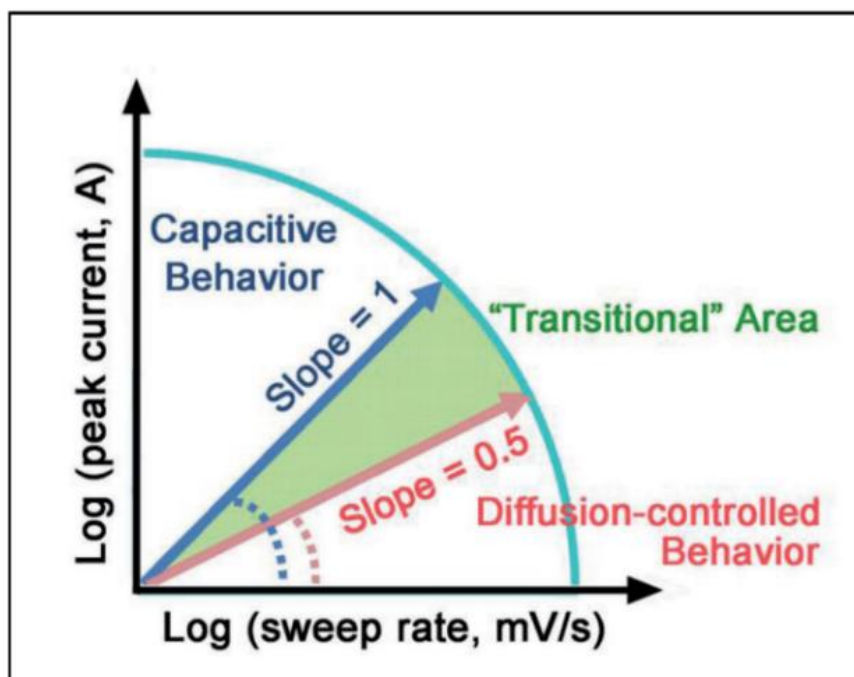**Figure 2.24** Power-law dependence of the peak current on sweep rate for capacitive materials (b= 1.0) and typical battery-type materials (b = 0.5). The "transition" area between capacitive and battery-type materials area is located in the range of b = 0.5–1.0. [23](Figure is taken from open access internet source)

Where i(V) is the current at a specific potential, sweep rates v. a and b are adjustable parameters, and the b value can be determined as the slope of log(i) vs log(v) for various sweep rates. When b = 1 is denoted surface control and 0.5 denoted diffusion control. When the b-value falls between 0.5 and 1, the mechanism is attributed to a combination of diffusion and capacitive contributions [151] b value presentation shown in **Figure 1.24.**

 Liu et al. proposed a linear combination of surface- and diffusion-controlled currents [24]

$$i(V) = k_1(V) v + k_2(V) v1/2 \tag{2.9}$$

Dunn et al. utilized this concept to deconvolute capacitive vs diffusive contributions to the total current for many types of nanostructured transition metal oxides. [25-27]

$$i(V)/v^{1/2} = k_1(V) \, v^{1/2} + k_2(V) \tag{2.10}$$

k_1 and k_2 determine surface and diffusion-controlled processes at specific potentials with multiple sweep rates. The method allows for the separation of the cyclic voltammograms into surface-controlled and diffusion-controlled regions.

Trasatti et al. developed another new method based on voltammetric charge to deconvolute the "inner" (less accessible) and "outer" (more accessible) surface contributions. [28]

According to **Trasatti,** voltammetric charge (Q) can be divided into surface-controlled and diffusion-controlled contributions,

$$Q = Qs + Qd \tag{2.11}$$

Where Qs and Qd are the surface-controlled and diffusion-controlled contributions to charge, respectively. Surface-controlled charge contribution also be divided into the "inner" surface contribution, Qs, in, and "outer" surface contribution,

$$Qs = Qs, \, in + Qs, \, out \tag{2.12}$$

The "inner" surface contribution is sweep rate dependent (due to lower accessibility of redox sites) and the outer" surface contribution is invariant of sweep rate, Assuming semi-infinite linear diffusion and a linear relationship between Q_d and $v^{-1/2}$, **equation (2.12)** can be rearranged to determine Qs, out when

$$Q = Q_{s, \, out} A1 = + v^{-1/2} \tag{2.13}$$

Where A1 is a constant. The y-intercept ($v^{-1/2} = 0$; or $v = \infty$) determines Qs. On the other hand, Qs is determined when $v = 0$. Assuming Q^{-1} decreases linearly with $v^{1/2}$, **equation 2,13** is rewritten as

$$Q^{-1} = Q_s^{-1} \, A_2 v^{1/2} \tag{2.14}$$

Where A_2 is another constant. Qs^{-1} can be obtained from the y-intercept ($v1/2 = 0$)

2.4.3.4 Charge-discharge (Chronopotentiometry)

Chronopotentiometry is used to study the mechanism and kinetics of chemical reactions. In this technique, the instrument operates in galvanostatic mode to control current and measure voltage. The applied current can consist of either a single or double step. It is generally performed in a quiet (unstirred) solution. This technique

can be used to investigate the mechanism of a redox process to observe where redox species are present.[29] The electrochemical theory should be consulted for a complete understanding of this method.

Consider the general reaction

$$O + ne^- \rightleftharpoons R \qquad (2.15)$$

with formal potential $E^{o'}$. As a constant current is applied to the working electrode, O is reduced to R at the working electrode surface. As a result, the working electrode potential moves to values characteristic of the redox couple in a time-based Nernstian fashion. As the concentration of O drops to zero at the electrode surface, the potential starts to rapidly increase to more negative values. The resulting $E - t$ curve is much like a potentiometric titration with a transition time, τ (analogous to titration equivalence point). The potential at one half τ is $E^{0'}$. The transition time is related to the concentration and diffusion coefficient of O through the expression

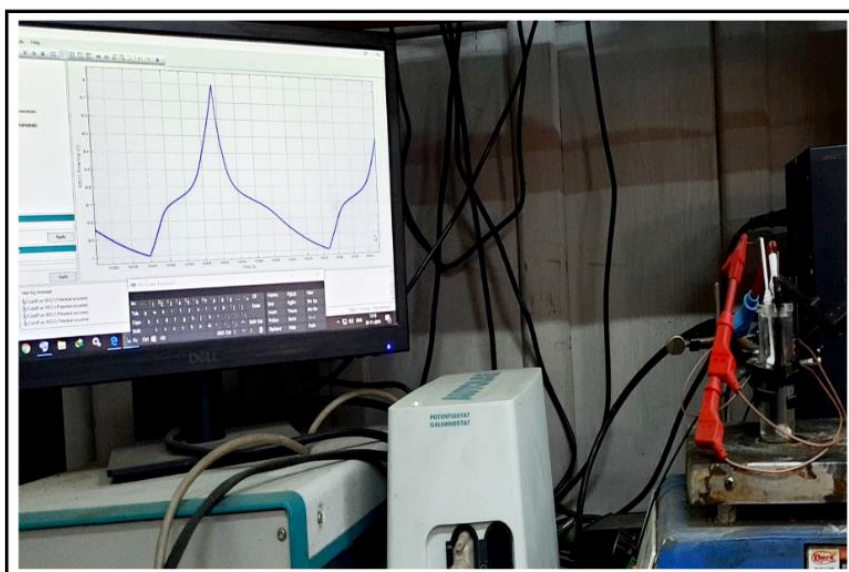$$\tau^{3/2} = \frac{2C_0^* n F A D_0^{1/2}}{3\beta} \qquad (2.16).$$

Figure 2.25: Charge-discharge (Chronopotentiometry) plot voltage vs. time

where C_0 is the concentration of O, n is the number of electrons, F is 96485C/F (Faraday's Constant), A is the working electrode area, D is the diffusion coefficient, and β is the sweep rate.

For rapid electrode kinetics, the time-based Nernstian equation is

$$E = E_{\tau/4} + \frac{RT}{nF} \ln \left(\frac{\tau^{1/2} - t^{1/2}}{t^{1/2}} \right)$$

(2.17)

where $E_{\tau/4}$ is equal to

$$E_{\tau/4} = E^{0'} - \frac{RT}{2nF} \ln \frac{D_O}{D_R}$$

(2.18)

A plot of E vs. $\ln \left(\frac{\tau^{1/2} - t^{1/2}}{t^{1/2}} \right)$ should give a straight line with a slope of RT/nF for a reversible $E - t$ curve [29-30] **Figure 2. 25** shows Charge-discharge (Chronopotentiometry) plot voltage vs. time.

2.4.3.5 Electrochemical Impedance Spectroscopy (EIS)

Electrochemical impedance spectroscopy (EIS) is the analytical method widely used to study electrochemical systems by applying a small AC voltage signal as a function of the frequency of the amplitude signal. In potentiostatic mode as that of direct current (DC) techniques, like Linear Polarization Resistance (LPR) or Polarization Potentiodynamic, the basic measurement parameter is the polarization resistance Rp that is equal to the impedance (Z) in alternate current (AC) mode. This can be represented according to the Ohm's Law equation as denote

R = V/I (DC) , Z = E/ I (AC)   (2.19)

where R is the resistor (Ω), V is the voltage (volts) and I is the current (amps) for direct current and E is the potential (volts) and Z is the impedance (Ω) for alternating current. To understand how the theory supports the EIS technique, it is necessary to consider two periodic waves; one is the current signal (I) and the other is related to the potential signal (E). These waves behave as that shown in Figure 3, in which both signals oscillate at the same frequency and intensity because one wave causes the other. However, there is an important effect that is the constant time shift between the

two waves at a certain angle, this is called the phase-angle shift (ϕ) and can vary from 0 to 90. Its unit is degrees (°), because usually waves are considered vectors in a polar coordinate system or a sine function.

As mentioned above, EIS data is usually represented by Bode plots in which the $|Z|$ module and phase angle ϕ are functions of the frequency domain, sustained by its complex plane form that relates to Z_{real} with the imaginary part Zim, and are usually interpreted by a mathematical correlation to a certain physico-electrical model known as equivalent electrical circuit (EEC), which is designed by an arrangement of ideal components (resistors R, capacitors C and inductors L) connected in series or parallel to reproduced the experimental EIS spectra [31-32]. In this study, a galvanostat potentiostat Autolab instrument (model no. PGSTAT204) was used to evaluate the effect of the voltage applied to the two-electrode interface. In which a periodic constant signal at 1 kHz of frequency was applied over a voltage range of 1 to 1000 mV as a function of the frequency domain (1 MHz to 1 mHz). **Figure 2.25** shows the impedance mechanism in a cole-cole plot.
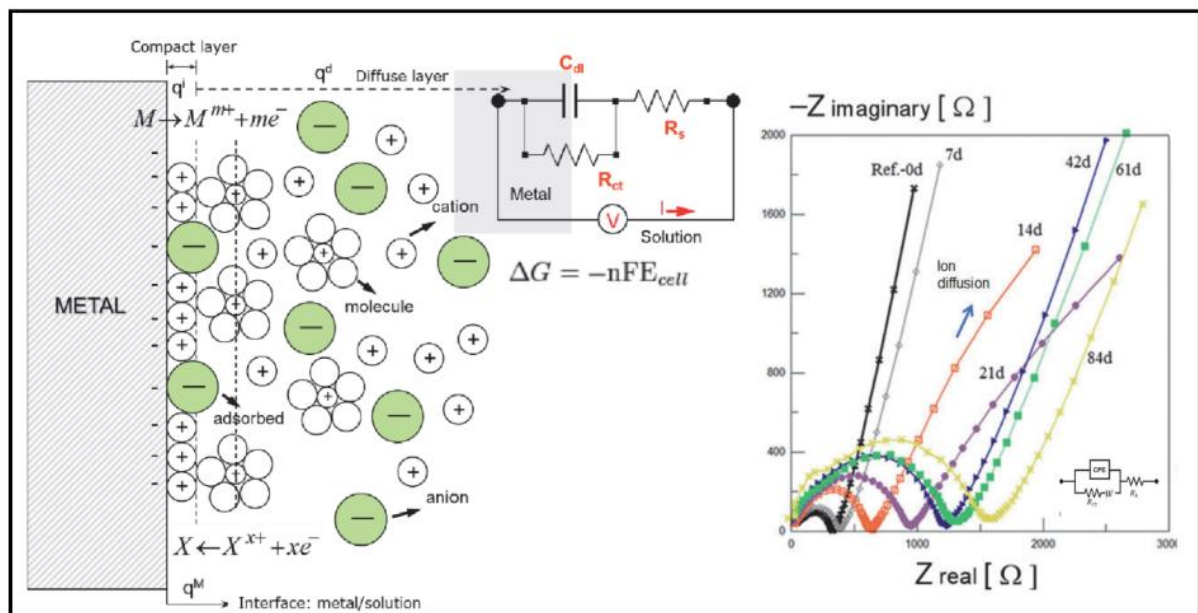

Figure 2.26: Electrochemical impedance spectroscopy (EIS) mechanism and cole-cole plot [31,32**]** (Figure is taken from open access internet source)